

See discussions, stats, and author profiles for this publication at: <https://www.researchgate.net/publication/233034319>

Bis(tetraisopropylcyclopentadienylnickel)dichalcogenide Complexes of the Novel $\{CpME\}_2$ Type (E = S, Se, Te)

ARTICLE in ORGANOMETALLICS · FEBRUARY 2001

Impact Factor: 4.13 · DOI: 10.1021/om000346i

CITATIONS

17

READS

23

5 AUTHORS, INCLUDING:



Helmut Sitzmann

Technische Universität Kaiserslautern

104 PUBLICATIONS 1,704 CITATIONS

SEE PROFILE



Axel Klein

University of Cologne

185 PUBLICATIONS 2,897 CITATIONS

SEE PROFILE



Roland Boese

University of Duisburg-Essen

987 PUBLICATIONS 15,299 CITATIONS

SEE PROFILE

Bis(tetraisopropylcyclopentadienylnickel)dichalcogenides: Complexes of the Novel $[(\text{Cp}^*\text{NiE})_2]$ Type (E = S, Se, Te)

Helmut Sitzmann,^{*,†} Dirk Saurenz,[†] Gotthelf Wolmershäuser,[†] Axel Klein,[‡] and R. Boese[§]

FB Chemie der Universität Kaiserslautern, Germany, Institut für Anorganische Chemie der Universität Stuttgart, Germany, and Institut für Anorganische Chemie der Universität-GH Essen, Germany

Received April 24, 2000

The dinuclear dichalcogenides $[(\text{C}_5\text{HR}_4\text{NiE})_2]$ (R = CHMe₂; E = S (**2**), Se (**3**), Te (**4**)) have been synthesized from $[(\text{C}_5\text{HR}_4\text{NiBr})_2]$ (**1**) (R = CHMe₂) and the corresponding disodium dichalcogenides. Crystal structure analyses show four-membered Ni₂E₂ rings with weak, but significant E...E interaction. **1–4** were characterized electrochemically and reveal nickel-centered oxidations, bridging ligand-centered reductions, and the formation of mixed-valent Ni(II)/Ni(III) species.

Introduction

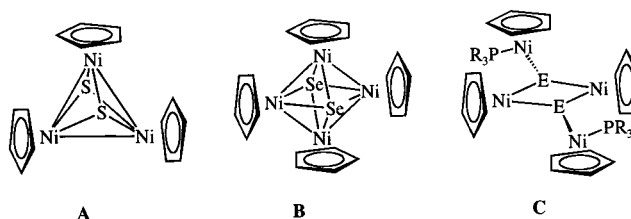
A great variety of dichalcogenide complexes have been studied since the seminal work of Hieber and Gruber¹ and the pioneering studies of Dahl and co-workers.² The majority of the crystallographically characterized complexes with E₂ ligands show E–E bond lengths shorter than the corresponding E–E single bonds (E = S, Se, Te), regardless of the coordination geometry and especially well documented for complexes with disulfur ligands.³

Several tri- and tetranuclear cyclopentadienylnickel complexes with two chalcogen atoms have been investigated by crystal structure determination (Scheme 1): $[(\text{CpNi})_3(\mu_3\text{-S})_2]$ (**A**),⁴ $[(\text{CpNi})_4(\mu_4\text{-E})_2]$ (**B**) (E = Se, Te),⁵ and $[(\text{CpNi})_2(\mu_3\text{-E})_2\{\text{Ni}(\text{PR}_3)\text{Cp}\}_2]$ (**C**) (E = Te, Se, R = Ph;⁵ E = S, R = Et⁶).

All these complexes show E...E distances much longer than E–E single bonds, but shorter than the sum of van der Waals radii. Are these contacts due to geometric constraints imposed on two nonbonded chalcogen atoms by up to four cyclopentadienylnickel bridges or are there E₂ ligands with significant E...E interaction?

Whereas dinuclear chalcogenides such as in situ generated $[(\text{C}_5\text{Me}_5\text{M})_2(\mu\text{-S})_2]$ (M = Ru, Rh, Ir) dimerize

Scheme 1. Cyclopentadienylnickel Chalcogenides



with formation of cubane clusters,⁷ we have evidence that a bulky cyclopentadienyl ligand like the tetraisopropyl derivative attached to nickel prevents the formation of any nuclearity higher than two and can therefore be expected to allow the preparation of the simple, yet unknown, $[(\text{Cp}^*\text{NiE})_2]$ type with E = S, Se, Te.

The thermally stable, but highly reactive cyclopentadienylnickel bromide dimer $[(\text{C}_5\text{HR}_4\text{Ni}(\mu\text{-Br}))_2]$ provides access to a variety of nickel half-sandwich complexes⁸ and has been used for the synthesis of nickel complexes with dichalcogenide ligands.

Results and Discussion

The dimeric cyclopentadienylnickel bromide derivative $[(\text{C}_5\text{HR}_4\text{Ni}(\mu\text{-Br}))_2]$ (**1**) reacts with 1 equiv of the sodium dichalcogenides Na₂E₂ with formation of the dimers $[(\text{C}_5\text{HR}_4\text{NiE})_2]$ (E = S [**2**], Se [**3**], Te [**4**]) in good yields (Scheme 2).

The compounds are well soluble in the common aprotic solvents and form crystals with metallic luster from petroleum ether solution. The color varies from grass green for the sulfur compound to forest green for the selenium and green-black for the tellurium derivative. Proton NMR spectra of **2–4** show the expected set of one singlet for the ring proton, two septets for two pairs of chemically equivalent methine protons, and four

* Corresponding author. FB Chemie der Universität, Erwin-Schrödinger-Str., D-67663 Kaiserslautern. Tel.: + 631/205-4399. Fax: + 631/205-4676. E-mail: sitzmann@chemie.uni-kl.de.

[†] FB Chemie der Universität Kaiserslautern.

[‡] Institut für Anorganische Chemie der Universität Stuttgart.

[§] Institut für Anorganische Chemie der Universität-GH Essen.

(1) Hieber, W.; Gruber, J. Z. Anorg. Allg. Chem. **1958**, 296, 91.
(2) Dahl, L. F.; Sutton, P. W. Inorg. Chem. **1963**, 2, 1067.
(3) Review articles: (a) Müller, A.; Jaegermann, W.; Enemark, J. H. Coord. Chem. Rev. **1982**, 46, 245. (b) Wachter, J. Angew. Chem. **1989**, 101, 1645; Angew. Chem., Int. Ed. Engl. **1989**, 28, 1613. (c) Wachter, J. Angew. Chem. **1998**, 110, 782; Angew. Chem., Int. Ed. Engl. **1999**, 37, 750. (d) Alvarez, S.; Palacios, A. A.; Aullón, G. Coord. Chem. Rev. **1999**, 185–186, 431.

(4) Neutral complex A: Vahrenkamp, H.; Uchtman, V. A.; Dahl, L. F. J. Am. Chem. Soc. **1968**, 90, 3272. Monocation: North, T. E.; Thoden, J. B.; Spencer, B.; Dahl, L. F. Organometallics **1993**, 12, 1299.

(5) Fenske, D.; Hollnagel, A.; Merzweiler, K. Angew. Chem. **1988**, 100, 978; Angew. Chem., Int. Ed. Engl. **1988**, 27, 965.

(6) Denninger, U.; Schneider, J. J.; Wilke, G.; Goddard, R.; Krüger, C. Inorg. Chim. Acta **1993**, 213, 129.

(7) Nagao, S.; Seino, H.; Okada, T.; Mizobe, Y.; Hidai, M. J. Chem. Soc., Dalton Trans. **2000**, 3546, and literature cited therein.

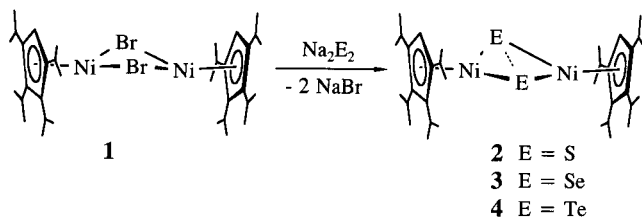
(8) Sitzmann, H.; Schär, M.; Saurenz, D.; Wolmershäuser, G.; Stalke, D.; Kärcher, J.; Dormann, E.; Winter, H.; Kelemen, M. Submitted for publication.

Table 1. Crystal Data and Summary of X-ray Data Collection^a for Complexes 1–4

	1 (lit. ⁸)	2	3	4
formula	C ₃₄ H ₅₈ Br ₂ Ni ₂	C ₃₄ H ₅₈ Ni ₂ S ₂	C ₃₄ H ₄₈ Ni ₂ Se ₂	C ₃₄ H ₅₈ Ni ₂ Te ₂
fw (g mol ⁻¹)	744.04	648.33	742.14	839.42
cryst size (mm)	0.70 × 0.40 × 0.30	0.3 × 0.2 × 0.1	0.34 × 0.27 × 0.17	0.43 × 0.38 × 0.14
space group	<i>P</i> 1	<i>C</i> 2/ <i>c</i>	<i>I</i> 2/ <i>a</i>	<i>P</i> 1
lattice params				
<i>a</i> (Å)	12.588(2)	18.737(4)	11.779(2)	12.769(1)
<i>b</i> (Å)	18.140(2)	17.779(2)	17.826(4)	18.238(1)
<i>c</i> (Å)	20.148(2)	11.733(4)	17.503(4)	20.453(2)
α (deg)	72.070(10)	90	90	107.63(1)
β (deg)	89.490(10)	115.038(9)	103.22(3)	90.77(1)
γ (deg)	85.650(10)	90	90	94.62(1)
<i>V</i> (Å ³)	4364.2(9)	3512.9(12)	3577.6(13)	4521.1(6)(2)
<i>Z</i>	10	4	4	5
<i>T</i> (K)	293(2)	293(2)	298(2)	293(2)
<i>D</i> _{calc} (g cm ⁻³)	1.416	1.388	1.378	1.542
μ (cm ⁻¹)	33.87	12.11	31.07	26.42
transmn factors	0.039–0.082	0.778–0.794	0.640–0.997	0.3963–0.7087
θ limits (deg)	2.04–19.52	2.02–27.50	1.50–25.00	2.02–25.00
total no. of rflns	8470	4201	3321	18 007
no. of ind rflns	7127	4199	3153	15 620
abs corr	semiempirical from ψ -scans	semiempirical from ψ -scans	semiempirical from ψ -scans	empirical
structure solution	direct methods	direct methods	direct methods	direct methods
program used	SIR92	SHELXTL	SHELXTL V.5.03	SHELXS-97
refinement	SHELXL-93	SHELXTL	SHELXTL V.5.03	SHELXL-97
no. of data/restraints/params	7126/0/914	3231/0/289	2359/0/163	15620/0/947
R1, wR2	0.0451, 0.0906 (<i>I</i> > 2 σ (<i>I</i>))	0.0685, 0.1130 (<i>I</i> > 2 σ (<i>I</i>))	0.0906, 0.2346 (<i>I</i> > 2 σ (<i>I</i>))	0.0391, 0.0803 (<i>I</i> > 2 σ (<i>I</i>))
R1, wR2 (all data)	0.0928, 0.1117	0.1507, 0.1431	0.1175, 0.2624	0.0691, 0.0911
Goof (all data)		1.060	1.014	1.016
max/min difference peak (e Å ⁻³)	0.387, -0.485	0.669, -0.	3.831, -1.950	0.472, -0.473

^a For all crystal structure determinations Mo K α radiation ($\lambda = 0.71073$ Å) has been used.

Scheme 2. Synthesis of Dichalcogenides 2–4



doublets arising from eight methyl groups. EI mass spectra have been obtained for the sulfur and selenium derivative **2** and **3** and show a signal for the dimeric molecular ion with 8.5% and 11.3% intensity.

The starting compounds contain Ni(II) and $(E_2)^{2-}$; therefore product formation could involve a redox reaction between E_2^{2-} as an oxidant and Ni(II) as a reductant. A distinction between the $(\mu, \eta^2: \eta^2-E_2)^{2-}$ moiety of a Ni(II) complex with an E–E single bond or two isolated $(\mu-E)^{2-}$ in a Ni(III) species cannot be derived from the analytical data; therefore crystal structure analyses and electrochemical measurements have been carried out on complexes **1–4**.⁹

The most detailed structural information regarding the Ni₂E₂ ring can be extracted from the data set of the ditellurium derivative **4** (Figure 1, Table 1). The unit cell is triclinic and closely resembles that of the bromo-bridged complex **1**.⁸ Like the bromo-bridged starting compound, the ditelluride crystallizes with five dimeric molecules in the unit cell and exhibits almost identical cell constants. Two pairs of dimers are related by inversion symmetry, and the fifth molecule is located on an inversion center itself.

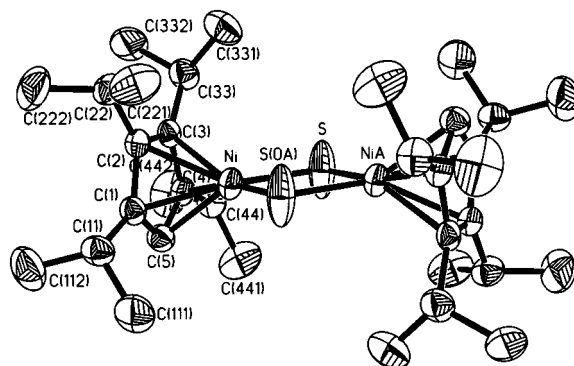


Figure 1. Crystal and molecular structure of [(C₅HR₄)-NiS]₂ (**2**) with atom-numbering scheme. Selected bond distances (Å) for disulfide **2**: S···S(0A) 2.745(2), Ni···NiA 3.241(2), Ni–S 2.129(2), Ni–S(0A) 2.120(2), Ni–C1 2.126(5), Ni–C2 2.130(5), Ni–C3 2.104(5), Ni–C4 2.089(5), Ni–C5 2.112(5), Ni–ring plane 1.732, ring C–C from 1.401(7) to 1.433(7), mean value 1.421. The angles S–Ni–S 80.57(7)° and Ni–S–Ni 99.43(7)° are probably not very meaningful; see discussion.

The Ni_2Te_2 core is contained between two almost parallel five-membered rings (interplanar angle 3.2°) and is bent with a fold angle along the $\text{Te}\cdots\text{Te}$ line of 165.4° . There is a disorder showing four half-occupied tellurium positions, with $\text{Te1A}\cdots\text{Te2A}$ occupying one Te_2 position, and $\text{Te3A}\cdots\text{Te4A}$ the second one. The $\text{Te}\cdots\text{Te}$ distance of 3.07 \AA (average of four $\text{Te}\cdots\text{Te}$ distances; the molecule on a center of symmetry has been omitted) is weaker than a full single bond (expected single bond length approximately 2.75 \AA ,¹⁰ cf. 2.835 \AA in hexagonal

(9) The crystal structure of complex **1** has been published in ref 8.

(10) Beck, J. *Coord. Chem. Rev.* **1997**, 163, 55.

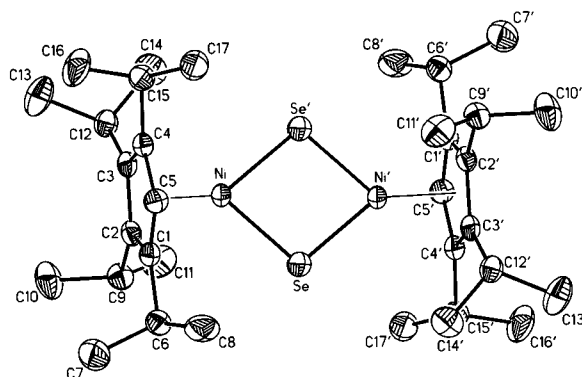


Figure 2. Crystal and molecular structure of $[(C_5HR_4)NiSe]_2$ (**3**) with atom-numbering scheme. Selected bond distances (Å) for diselenide **3**: Se \cdots Se' 2.855(2), Ni \cdots Ni' 3.457(2), Ni–Se 2.248(2), Ni–Se' 2.237(2), Ni–C1 2.131(6), Ni–C2 2.127(6), Ni–C3 2.106(6), Ni–C4 2.098(6), Ni–C5 2.113(6), Ni1A–ring plane 1.739, Ni2A–ring plane 1.742, ring C–C distances from 1.405(6) to 1.461(6), mean values 1.435 for C1A–C5A and 1.434 for C6A–C10A. The angles Se–Ni–Se 79.21(6)° and Ni–Se–Ni 100.79(6)° are probably not very meaningful; see discussion.

tellurium)¹¹ and may be regarded as a long bond slightly shorter than the 3.12 Å bond length in the trigonal prismatic Te_6^{4+} cation¹² and slightly longer than the 2.993 Å bond distance in the Te_6^{2+} cation.¹³ The Te \cdots Te distance of 3.28 Å in $[(C_5H_5)Ni]_2(\mu_3-Te)_2\{Ni-(PPh_3)(C_5H_5)\}_2$ (Scheme 1, type **C**) is significantly longer and has been interpreted as a bonding interaction.⁵ A clearly nonbonding situation can be seen, for example, in $[(C_5H_4CMe_3)_2Zr(\mu-Te)]_2$ with a Te \cdots Te distance of 4.006(1) Å.¹⁴ The distance between the nickel atoms of **4** is nonbonding with 3.765 Å (average of two bond lengths, the molecule on a center of symmetry has been neglected).

For **2** and **3** the disorder of the chalcogen atoms could not be resolved, leaving cigar-shaped thermal ellipsoids (Figures 2 and 3). The molecular structure most likely consists of a puckered four-membered ring in analogy with the tellurium example discussed in the preceding paragraph. The Ni–E(center of ellipsoid) distances cannot be taken as Ni–E bond lengths, because the center of the chalcogen ellipsoids is not the actual position of the respective atom. The E \cdots E distances, however, are more meaningful, because the long axes of the thermal ellipsoids in both cases are generated by a parallel shift in a direction perpendicular to the E \cdots E vector under consideration.

Molecules of both **2** and **3** are located on a crystallographic center of symmetry, and the Ni_2E_2 core is situated between two parallel and ideally staggered tetraisopropylcyclopentadienyl ligands. All four isopropyl groups stretch their methine C–H bond roughly parallel to the ring plane, one methyl group above and

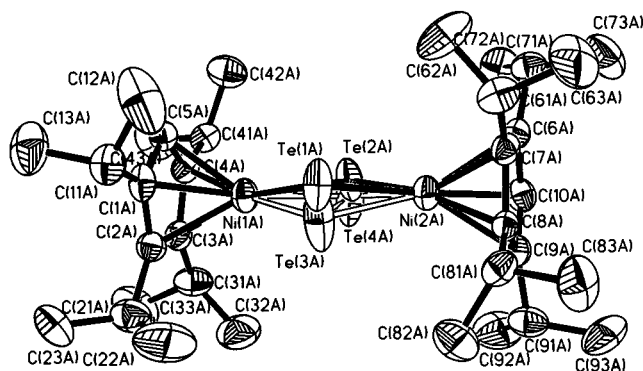


Figure 3. Crystal and molecular structure of $[(C_5HR_4)NiTe]_2$ (**4**) with atom-numbering scheme. Selected bond distances (Å) for ditelluride **3** (molecule A): Te1A \cdots Te2A 3.052(5), Ni1A \cdots Ni2A 3.788(4), Ni1A–Te1A 2.438(3), Ni1A–Te2A 2.449(4), Ni2A–Te1A 2.448(3), Ni2A–Te2A 2.442(4), Ni1A–ring plane 1.739, Ni2A–ring plane 1.742, ring C–C distances from 1.405(6) to 1.461(6), mean values 1.435 for C1A–C5A and 1.434 for C6A–C10A.

one below the ring plane. The two isopropyl groups in 1- and 4-position of each ring are oriented with their methyl groups toward the only substitution gap of the ring (the ring CH group). These two features are common to all tetraisopropylcyclopentadienyl complexes structurally characterized so far. Like the centrosymmetric dimer $[(C_5HR_4)Co(\mu-Cl)]_2$ of the same type,¹⁵ **2** and **3** show ring CH groups not rotated into the four-membered ring plane, but above and below that plane. The extra space provided by these gaps is obviously not needed by the chalcogen atoms. These are on one side accommodated by two isopropyl groups properly turned away from each other and face the full bulk of the second ring on the other side. This results in only slightly unsymmetric bridging and an E_2 orientation not exactly perpendicular to the Ni \cdots Ni vector. The Ni \cdots Ni distance of 3.241(2) Å is nonbonding, and the S \cdots S distance of 2.745(2) Å is much longer than a single bond (2.05 Å in S_8), but significantly shorter than the long transannular S \cdots S interaction in S_8^{2+} (2.83 Å¹⁶), the closest contact of two (μ_3 -S) ligands in $[(C_5H_5)Fe(\mu_3-S)]_4$ ¹⁷ ($n = 0$: 2.874(10) Å; $n = +1$: 2.879(6) Å),¹⁷ or the S \cdots S distance of 2.86 Å in centrosymmetric $[(C_5H_5)Ni(\mu_3-S)]_4$.¹⁸ It has been noted that the S \cdots S distance of 3.005(2) Å found in $[(dppp)_2Pt(\mu-S)]_2$ (dppp = 2-diphenylphosphinopyridine) is comparable to the distances found in bidentate thioether complexes and related compounds.¹⁹

For the selenium derivative **3** the Ni \cdots Ni distance is 3.457(2) Å and nonbonding. The Se \cdots Se distance of 2.855(2) Å is again much longer than a single bond (cf. 2.374 Å for hexagonal selenium)¹¹ and can be compared with the transannular interaction in cyclic Se_8^{2+} (2.84

(11) Steudel, R. *Chemie der Nichtmetalle*, 2nd ed.; Walter de Gruyter: Berlin, 1998; p 278.

(12) $Te_6[AsF_6]_4$: Burns, R. C.; Collins, M. J.; Luk, W.-C.; Slim, D. R. *Inorg. Chem.* **1979**, *11*, 3086. $(Te_6)(Se_6)[AsF_6]_6 \cdot SO_2$: Collins, M. J.; Gillespie, R. J.; Sawyer, J. F. *Acta Crystallogr. C* **1988**, *44*, 405.

(13) $Te_8[WCl_6]_2$: Beck, J. *Angew. Chem.* **1996**, *109*, 301; *Angew. Chem., Int. Ed. Engl.* **1996**, *36*, 293. $Te_8[ReCl_6]_2$: Beck, J.; Müller-Buschbaum, K. *Z. Anorg. Allg. Chem.* **1997**, *623*, 409.

(14) Erker, G.; Nolte, R.; Tainturier, G.; Rheingold, A. *Organometallics* **1989**, *8*, 454.

(15) $[(C_5HR_4)Co(\mu-Cl)]_2$ (R = CHMe₂): Baumann, F.; Dormann, E.; Ehleiter, Y.; Kaim, W.; Kärcher, J.; Kelemen, M.; Krammer, R.; Saurenz, D.; Stalke, D.; Wachter, C.; Wolmershäuser, G.; Sitzmann, H. *J. Organomet. Chem.* **1999**, *587*, 267.

(16) Davies, C.; Gillespie, R. J.; Park, J. J.; Passmore, J. *Inorg. Chem.* **1971**, *10*, 2781.

(17) Neutral complex: Wei, C. H.; Wilkes, T. R.; Treichel, P. M.; Dahl, L. F. *Inorg. Chem.* **1966**, *5*, 900. Cation: Trinh-Toan; Fehlhammer, W. P.; Dahl, L. F. *J. Am. Chem. Soc.* **1977**, *99*, 402.

(18) Vahrenkamp, H.; Dahl, L. F. *Angew. Chem.* **1969**, *81*, 152; *Angew. Chem., Int. Ed. Engl.* **1969**, *8*, 144.

(19) Yam, V. W.-W.; Yeung, P. K.-Y.; Cheung, K.-K. *J. Chem. Soc., Chem. Commun.* **1995**, 267, and literature cited therein.

Table 2. Electrochemical Data^a of Nickel Complexes $[(C_5HR_4)NiX]_2$ 1–4

compound	$E_{1/2}(oxII)$ (ΔE_p) ^b	$E_{1/2}(oxI)$ (ΔE_p) ^b	$E_{1/2}(redI)$ (ΔE_p) ^b	$E_{1/2}(redII)$ (ΔE_p) ^b	solvent/temp
1	0.09 ^c	–0.13 (68)			CH ₂ Cl ₂
X = Br	0.29 ^c				
	0.10 (73)	–0.17 (66)			CH ₂ Cl ₂ /–40 °C
	0.26 (84)	–0.04 (73)			THF/–30 °C
2	0.46 (80)	–0.37 ^c			CH ₂ Cl ₂
X = S		–0.11 ^c			
	0.44 irr. ^d	–0.08 (80)	–1.71 (83)	–2.76 irr. ^e	THF
3	0.35 (64)	–0.17 (63)	–1.79 irr. ^e		CH ₂ Cl ₂
X = Se	0.32 (84)	–0.02 (87)	–1.68 (78)	–3.99 irr. ^e	THF
4	0.17 (71)	–0.27 (63)	–1.62 (81)		CH ₂ Cl ₂
X = Te	0.11 (83)	–0.11 (78)	–1.66 (75)	–2.83 irr. ^e	THF
	0.08 (65)	–0.14 (68)	–1.65 (78)	–2.72 (83)	THF/–10 °C

^a From cyclic voltammetry of square-wave voltammetry in 0.1 M Bu₄NPF₆ solutions, scan rate 100 mV/s. The ferrocene/ferrocenium couple served as internal reference. ^b Half-wave potentials $E_{1/2}$, peak potential differences $\Delta E_p = E_{pa} - E_{pc}$ in mV in parentheses. ^c Anodic peak potentials E_{pa} for oxidations (below) or cathodic peak potentials E_{pc} (above) for corresponding reduction steps. ^d Anodic peak potentials for irreversible oxidations. ^e Cathodic peak potentials for irreversible reductions.

Å).²⁰ It is considerably shorter than the Se···Se interaction in $[(C_5H_5)Ni]_2(\mu_3\text{-Te})_2[(C_5H_5)NiPPh_3]_2$ (3.117(1) Å, Scheme 1, type **C**) or in $[(C_5H_5)Ni]_4(\mu_4\text{-Te})_2$ (3.053(1) Å, Scheme 1, type **B**), for which a bonding interaction has been discussed.⁵

Complexes of type **C** (Scheme 1) are closely related to the dinuclear compounds **2–4**. In a formal sense (and neglecting the different Cp substituent pattern) those complexes can be converted to the $[(CpNiE)_2]$ type by $\{CpNiPR_3\}$ fragment removal. In all three cases the E···E interaction is strengthened with this hapticity decrease from $\mu_3\text{-E}$ to $\mu_2\text{-E}$: The E···E distances in **2**, **3**, and **4** are shorter by 6.0, 8.4, and 6.4% than those found in the tetranuclear derivatives of type **C** (Scheme 1).

The substituent pattern is, however, not arbitrary: If complexes of the $[(CpNiE)_2]$ type were available with Cp = C₅H₅, they should be known already. The reaction of $[(C_5H_5)_2Ni(\mu\text{-CO})_2]$ with elemental sulfur gives nickel sulfides and nickelocene as main products.¹⁸

Complexes **2–4** appear to be the only known chalcogenides of the type $[(CpME)_2]$ (Cp = substituted or unsubstituted cyclopentadienyl ligand, M = transition metal, E = chalcogen). Even if we allow pnictogens for E, only one example, again with tetraisopropylcyclopentadienyl ligands, is known: $[(C_5HR_4)NiP]_2$ (R = CHMe₂).²¹ With less sterically demanding ring substituents higher nuclearity complexes have been observed, e.g., the cubane compounds $[(C_5H_4CMe_3)NiP]_4$ ²² and $[(C_5H_4Me)Ni]_4(\mu_3\text{-E})_4$ (E = P, As).²³ Even with pentamethylcyclopentadienyl ligands cubane type complexes with three $\{(C_5Me_5)Ni\}$ fragments $[(C_5Me_5)Ni]_3(\mu_3\text{-E})$ ($\mu_3, \eta^1\text{-}\eta^1\text{-}\eta^1\text{-E}_4$) (E = P, As) have been structurally characterized.²³

With tetraisopropylcyclopentadienyl ligands coordinated to nickel even the ditellurium derivative **4** offers no space for a third bulky fragment like this. Therefore, **2–4** can be obtained in good yield without concomitant formation of higher oligomers.

Among the three dichalcogenide ligands discussed here the element–element interaction has been found

weakest for sulfur and strongest for tellurium and reflects the electronegativity difference within this series. The electron-withdrawing effect of the ligands is expected to be highest in the sulfur derivative with almost complete cleavage of the disulfide ligand in two separated sulfide ligands. The reverse is true for the tellurium derivative. The selenium compound occupies an intermediate position. The E···E distances could be the result of weak E···E bonding, but they could also be the result of steric strain: The repulsion between the E atoms and the bulky tetraisopropylcyclopentadienyl ligands shifts the $[(C_5HR_4)Ni]$ fragments apart (there is no Ni–Ni bond), with Ni···Ni distances increasing from E = S to E = Te. The strong Ni–E bonds are the “hard” parameters in this process, and consequently the E···E distances are determined by geometric requirements.

These ideas call for an investigation of electrochemical behavior, which should provide more insight into the electronic nature of dichalcogenides **2–4** (Table 2).

The first reduction step is reversible in THF for all three dichalcogenides; in methylene chloride only for **3** and **4**. It is attributed to the dichalcogenide bridge, because a comparable reduction step could not be observed for the bromo complex **1**. (The reverse interpretation also makes sense, however: If we reduce Ni(III) to Ni(II), we do not expect a similar reduction for bromide **1**, because **1** does not contain Ni(III).) This one-electron reduction takes place at increasingly negative potentials from the ditelluride **4** to the disulfide **2** (Table 2). A second one-electron reduction can be observed in THF at strongly negative potentials. It is not reversible at room temperature, but reversible at –10 °C for the tellurium derivative **4** and is also attributed to the dichalcogenide bridge or to reduction of the second Ni(III) center.

The dianions are extremely strong reducing agents which obviously decompose in solution at room temperature, probably due to loss of tetraisopropylcyclopentadienyl anion.

All four complexes show two reversible one-electron oxidation steps, which presumably correspond to subsequent oxidation of two nickel centers. For **2–4**, however, this could also be the oxidation of two bridging E^{2–} ligands to one E₂^{2–} bridge. Although oxidation of the disulfide **2** is hampered by strong adsorption to the working electrode, **2** has been found to exhibit the

(20) Mullen, R. K.; Price, D. J.; Corbett, J. D. *Inorg. Chem.* **1971**, *10*, 1749.

(21) Scherer, O. J.; Braun, J.; Walther, P.; Heckmann, G.; Wolmershäuser, G. *Angew. Chem.* **1991**, *103*, 861; *Angew. Chem., Int. Ed. Engl.* **1991**, *30*, 852.

(22) Scherer, O. J.; Dave, T.; Wolmershäuser, G. *J. Organomet. Chem.* **1988**, *350*, C20.

(23) Scherer, O. J.; Braun, J.; Wolmershäuser, G. *Chem. Ber.* **1990**, *123*, 471–475.

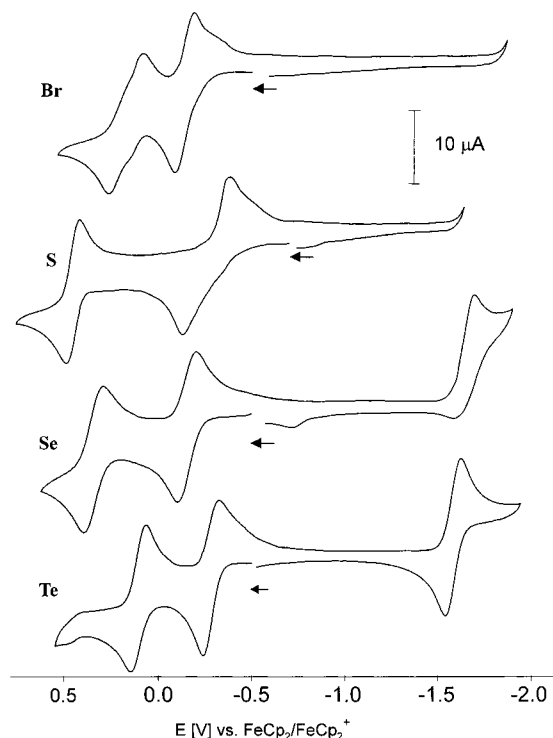


Figure 4. Cyclic voltammograms of complexes **1–4**, measured in 0.1 M Bu₄NPF₆/dichloromethane at ambient temperature and 100 mV/s scan rate. The second oxidation step for the bromide dimer **1** is not reversible, as indicated by the fairly large separation of 200 mV for oxidation and reduction wave (see Table 2). The shoulders are most likely due to adsorption processes at the electrode (see text); an as yet unknown side product cannot be ruled out, however.

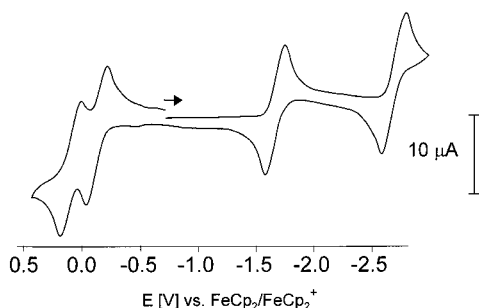
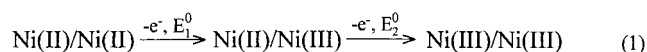


Figure 5. Cyclic voltammogram of complex **4**, measured in 0.1 M Bu₄NPF₆/thf at -10°C and 100 mV/s scan rate.

largest potential gap between the two individual oxidation steps (probably more than 0.6 V, see Table 2). The comproportionation constants K_c according to eqs 1 and 2 for the mixed-valent Ni(II)/(III) species are calculated to 6.81×10^{11} for E = S, 6.17×10^8 for E = Se, 2.74×10^7 for E = Te, and 2.57×10^5 for E = Br (all calculated from redox potentials obtained in CH₂Cl₂ solution; Table 2).



$$K_c = \frac{[\text{Ni(II)/Ni(III)}]^2}{[\text{Ni(II)/Ni(II)}][\text{Ni(III)/Ni(III)}]} = \exp\left[\frac{(E_1^0 - E_2^0)F}{RT}\right] \quad (2)$$

The complexes **2–4** appear to be neither Ni(II) complexes with an E₂²⁻ bridge nor Ni(III) complexes with two E²⁻ bridges. The diamagnetism of **2–4** in

contrast to the paramagnetism of **1** supports this interpretation. The oxidation state formalism is not appropriate in this case, and delocalized molecular orbitals with contributions from nickel and chalcogen atoms have to be considered. For more profound assignment of the redox sites we embarked on spectroelectrochemical and theoretical investigations, which will provide detailed characterization and classification of the mixed-valent species according to Robin and Day²⁴ and will be reported on in due course.

Considering the high reactivity of **1** and the possible catalytic activity of disulfide complexes in general,²⁵ the dichalcogenides **2–4** presented here might also turn out to be valuable starting compounds for a range of follow-up reactions.

Summary

The dichalcogenide bridges of the dinickel complexes [(C₅HR₄)Ni]₂(μ,η²:η²-E₂) (R = CHMe₂, E = S, Se, Te) with weak E...E interaction comparable to the long bonds found in polyatomic cations of sulfur, selenium, or tellurium fall right into the gap between the majority of E₂ ligands with rather short E–E bond lengths and (E)₂ complexes with nonbonding distances between the chalcogenide atoms. Electrochemical experiments have shown that all compounds undergo two separate one-electron oxidation reactions and revealed the occurrence of mixed-valent intermediates. The dichalcogenide-bridged complexes show additionally one (**2**, **3**) or two (**4**) reversible reduction steps. An unambiguous description of bonding in **2–4** requires further experimental and theoretical work.

Experimental Section

All synthetic operations were performed under a dry dinitrogen atmosphere following conventional Schlenk or drybox techniques. Tetrahydrofuran and petroleum ether (boiling range 40–60 °C) were distilled from potassium metal. NMR spectra were taken on a Bruker AMX 400 MHz spectrometer. Chemical shifts are given in ppm and refer to the appropriate solvent signals. Mass spectra were taken on a Finnigan MAT 90 mass spectrometer.

Electrochemical experiments were carried out in 0.1 M Bu₄NPF₆ solutions using a three-electrode configuration (glassy carbon working electrode, Pt counter electrode, Ag/AgCl reference) and a PAR 273 potentiostat and function generator. The ferrocene/ferrocenium couple served as internal reference. The number of electrons involved in the various processes was adjusted using weighed samples of ferrocene. Cyclic voltammetry was carried out at 100 mV/s scan rate. Square-wave voltammetry was performed with the following parameters: scan rate 15 mV/s, incr. 2 mV, freq 10 Hz. Peak potential differences ΔE_p found in THF solution are consistently higher than the theoretical value of 59 mV. This is mainly due to insufficient *iR*-drop compensation in such an unpolar solvent.^{26,27}

General Synthetic Procedure. To a red-brown tetrahydrofuran solution of the dimeric bromide **1** cooled in an acetone/dry ice bath is added 1 equiv of the solid disodium

(24) Robin, M. B.; Day, P. *Adv. Inorg. Chem. Radiochem.* **1967**, *10*, 247.

(25) Rakowski DuBois, M. *Chem. Rev.* **1989**, *89*, 1.

(26) Geiger, W. E.; Hawley, M. D. In *Physical Methods of Chemistry*, Vol. III, 2nd ed.; *Electrochemical Methods*; Rossiter, B. W., Hailton, J. F., Eds.; John Wiley & Sons: New York, 1986; pp 1–52.

(27) Osteryoung, J. *Acc. Chem. Res.* **1993**, *26*, 77.

Table 3. Experimental Details Regarding the Preparation of Complexes 2–4

complex	ingredients	isolated yield	formula	analysis calcd	analysis found
2	1: 242 mg (0.392 mmol) Na ₂ S ₂ : 44 mg (0.399 mmol)	145 mg (0.224 mmol; 57.1%)	C ₃₄ H ₅₈ Ni ₂ S ₂ MW 648.083	62.98% C 9.02% H	63.15% C 9.26% H
3	1: 500 mg (0.672 mmol) Na ₂ Se ₂ : 137 mg (0.672 mmol)	420 mg (0.566 mmol; 84.2%)	C ₃₄ H ₅₈ Ni ₂ Se ₂ MW 742.620	55.03% C 7.88% H	55.26% C 7.91% H
4	1: 220 mg (0.295 mmol) Na ₂ Te ₂ : 88 mg (0.292 mmol)	165 mg (0.196 mmol; 67.3%)	C ₃₄ H ₅₈ Ni ₂ Te ₂ MW 839.900	48.65% C 6.96% H	48.77% C 7.05% H

dichalcogenide Na₂E₂. The magnetically stirred mixture is kept for 30 min at dry ice temperature, then allowed to warm slowly to room temperature overnight. Removal of the solvent in vacuo is followed by petroleum ether extraction of the black residue. After filtration or centrifugation the petroleum ether solution is concentrated until incipient crystallization is observed, then placed in a freezer at –85 °C. Experimental details are compiled in Table 3.

2: Mp: 145 °C. Anal. Calcd for C₃₄H₅₈Ni₂S₂: C, 63.15; H, 9.26. Found: C, 62.98; H, 9.02. ¹H NMR (CDCl₃, 400 MHz): δ 4.74 (s, 2H, ring-CH), 2.94 (sep, 4 H, CHMe₂), 2.84 (sep, 4 H, CHMe₂), 1.42 (d, 12 H, J_{HH} = 7.0 Hz, CH₃), 1.36 (d, 12 H, J_{HH} = 6.8 Hz, CH₃), 1.20 (d, 12 H, J_{HH} = 7.0 Hz, CH₃), 1.05 (d, 12 H, J_{HH} = 6.8 Hz, CH₃). MS (EI, 70 eV; m/z (%)): 645 ([M]⁺, 8.5); 234 ([C₁₇H₃₀]⁺, 11.9); 217 ([C₁₆H₂₇]⁺, 14.8); 149 ([C₁₁H₁₇]⁺, 11.9); 107 ([C₈H₁₁]⁺, 100); 43 ([C₃H₇]⁺, 55.5).

3: Mp: 171 °C. Anal. Calcd for C₃₄H₅₈Ni₂Se₂: C, 55.26; H, 7.91. Found: C, 55.03; H, 7.88. ¹H NMR (CDCl₃, 400 MHz): δ 4.77 (s, 2H, ring-CH), 3.00 (sep, 4 H, CHMe₂), 2.89 (sep, 4 H, CHMe₂), 1.44 (d, 12 H, J_{HH} = 6.9 Hz, CH₃), 1.38 (d, 12 H, J_{HH}

= 6.5 Hz, CH₃), 1.21 (d, 12 H, J_{HH} = 6.9 Hz, CH₃), 1.06 (d, 12 H, J_{HH} = 6.5 Hz, CH₃). MS (EI, 70 eV; m/z (%)): 741 ([M]⁺, 11.3); 234 ([C₁₇H₃₀]⁺, 8.5); 43 ([C₃H₇]⁺, 100).

4: Mp: 201 °C. Anal. Calcd for C₃₄H₅₈Ni₂Te₂: C, 48.77; H, 7.05. Found: C, 48.65; H, 6.96. ¹H NMR (CDCl₃, 200 MHz): δ 4.67 (s, 2H, ring-CH), 2.89 (sep, 4 H, CHMe₂), 2.87 (sep, 4 H, CHMe₂), 1.42 (d, 12 H, J_{HH} = 7.2 Hz, CH₃), 1.25 (d, 12 H, J_{HH} = 6.8 Hz, CH₃), 1.20 (d, 12 H, J_{HH} = 7.2 Hz, CH₃), 1.06 (d, 12 H, J_{HH} = 6.8 Hz, CH₃).

Acknowledgment. H.S. is grateful to Prof. O. J. Scherer for generous support. Thanks are also given to the Deutsche Forschungsgemeinschaft for financial support (Grant Si 366/9-1, 9-2).

Supporting Information Available: This material is available free of charge via the Internet at <http://pubs.acs.org>.

OM000346I